Pergamon

1350-4495(94)00083-2

Infrared Phys. Technol. Vol. 36, No. 1, pp. 427–438, 1995

1350-4495/95 $9.50 + 0.00

RECENT PROGRESS IN TUNABLE NONLINEAR OPTICAL DEVICES FOR INFRARED SPECTROSCOPY

U. SIMON and F. K. TITTEL

Department of Electrical and Computer Engineering, Rice University, P.O. Box 1892, Houston, TX 77251, U.S.A.

(Received 27 May 1994)

Abstract—A laser source based on difference-frequency generation (DFG) in $AgGaS_2$ has been developed for high resolution IR kinetic spectroscopy (IRKS) of free radicals. Continuously tunable radiation has been generated between 4 and 9 μm (2500–1100 cm^{-1}) by mixing two cw single-mode dye/Ti:Al_2O_3 lasers in a 90° type I phasematching configuration. Spectra of the free radicals HOCO, DOCO and HCCN were obtained by using this source.

Concurrently, the suitability of III-V single-mode cw diode lasers for DFG of tunable IR radiation has been explored by mixing two laser diodes (808 and 690 nm) in $AgGaS_2$ (IR power generated ≈ 3 nW). Techniques to increase the IR DFG power level such as the use of high-power optical semiconductor amplifiers or an external build-up cavity for the nonlinear crystal have been investigated. As much as 50 μW of cw IR radiation, tunable near 4.3 μm have been generated by mixing a high-power tapered semiconductor amplifier at 858 nm and a Ti:Al_2O_3 laser in $AgGaS_2$. Recent progress in generating cw IR radiation near 3.2 μm by mixing an extended-cavity diode laser near 795 nm and a compact diode-pumped Nd:YAG laser in $AgGaS_2$ with an external enhancement cavity is also described.

I. INTRODUCTION

Ever since the invention of the laser there has been a great deal of interest in the development of efficient continuously tunable single-mode light sources. Particularly attractive for spectroscopic applications is the IR fingerprint region from 2 to 20 μm since the vast majority of molecules has IR active vibrations in this wavelength region. CW sources have the greatest potential for providing an optimum combination of spectral control and frequency stability. Although cw tunable laser sources, such as color center lasers, lead-salt diode lasers, and CO and CO_2 sideband lasers exist in this spectral region, each type of laser suffers from practical drawbacks such as requirement of cryogenic cooling, operational wavelength ranges which do not reach regions of great interest, incomplete coverage of their nominal operational wavelength range, and lack of portability and ruggedness.

DFG in a suitable nonlinear optical medium offers a viable alternative to traditional IR laser sources, especially when wide tunability is desired. The spectroscopic source originally developed by Pine[1] in which an Ar^+ laser is mixed with a cw dye laser in $LiNbO_3$ has proved very useful for high-resolution spectroscopy, but was limited to wavelengths shorter than 4 μm by the IR transmission characteristics of the nonlinear material $LiNbO_3$. Using $LiIO_3$ as the nonlinear medium, Oka and coworkers[2] extended the long wavelength limit for cw DFG spectroscopic sources to nearly 5 μm.

Advances in the growth and fabrication of the nonlinear optical materials $AgGaS_2$ and $AgGaSe_2$, now offer a convenient means for extending the wavelength coverage of DFG sources to a wider wavelength range (3–18 μm). Recently, we demonstrated the operation of a tunable cw DFG spectrometer in the 4–9 μm region based on type I noncritical phasematching in $AgGaS_2$ pumped by two single-mode dye/Ti:Al_2O_3 lasers.[3,4] This spectrometer extends the advantages of DFG sources into the chemically interesting "fingerprint" region of the IR, greatly increasing its applicability. This source is the essential element of an IRKS apparatus designed to investigate

molecular free radicals. In the following we discuss the $AgGaS_2$ DFG spectrometer; the observation of HOCO, DOCO and HCCN; and experiments involving DFG in $AgGaS_2$ using III–V diode lasers as pump laser sources. The use of semiconductor diode lasers as pump sources in DFG[5,6] is particular attractive, as their compact size and ease-of-operation allow the construction of a portable and robust mid-IR laser source especially suitable for environmental remote sensing, pollution monitoring, chemical analysis and medical research.

II. DFG SOURCE AS A PROBE SOURCE FOR IRKS

IRKS has proven to be a powerful tool for studying the spectroscopy of free radicals and for following their chemical kinetics[7] since every polyatomic molecule (with the exception of homonuclear diatomics) has at least one IR active absorption. The real power of this technique lies in its ability to distinguish between different absorbing species by frequency and/or temporal discrimination. IRKS can achieve detectivities of 10^{-3} (0.1% absorption for trace gas species) of number densities as low as 10^{-12} molecules cm^{-3}.

The $AgGaS_2$ DFG spectrometer, shown in Fig. 1 has been described in detail previously.[3,4] Two cw single-mode dye/Ti:Al_2O_3 ring lasers ($\delta\lambda \approx 1$ MHz) are pumped by the all-lines output of a high-power Ar^+ laser, typically operated at ~ 19 W. One ring laser (Coherent 899-21) is operated in a dye cavity configuration lasing on DCM-special dye and provides the pump beam ($\lambda \approx 620$–690 nm). The second ring laser (Coherent 899-29) is operated in a Ti:Al_2O_3 cavity configuration and provides the signal beam ($\lambda \approx 700$–850 nm). Pump and signal beams are polarized perpendicular for 90° type I phasematching and are spatially overlapped with a polarizing beam splitter. The copropagating beams are focused into a 45 mm long $AgGaS_2$ crystal (Cleveland Crystals, Inc.) cut for 90° type I phasematching to a beam waist of $\sim 40\ \mu m$. The generated IR radiation is collimated and propagates through a ZnSe beamsplitter. A small portion of the IR light passes through a 20 cm reference gas cell and is monitored by a liquid-N_2-cooled HgCdTe detector. The main portion of the IR traverses an absorption cell (White cell design) and is monitored by a second HgCdTe detector. The excimer laser radiation used to create the transient radical population enters one end of the White cell and overlaps the IR probe beam. Germanium filters with antireflective IR coatings are placed in front of each detector to eliminate the residual visible and UV laser light.

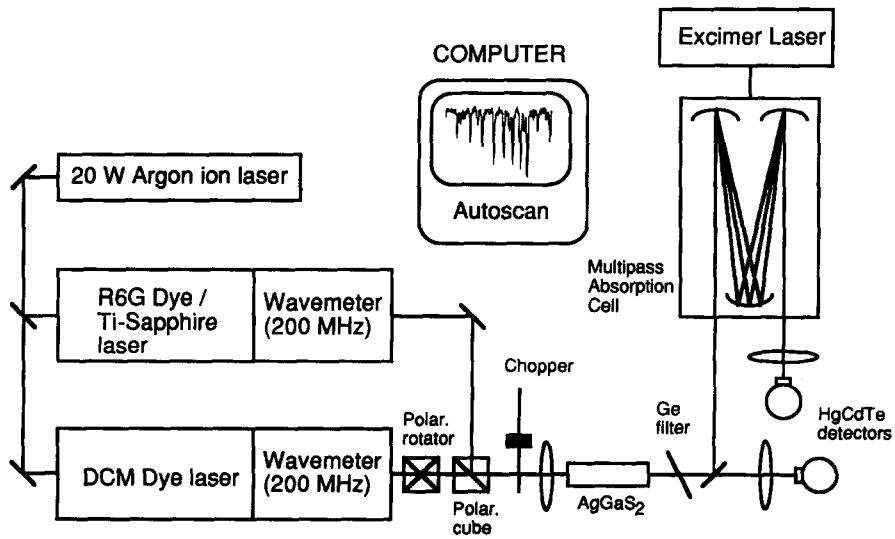

Fig. 1. Schematic experimental setup of the $AgGaS_2$ DFG spectrometer (3–9 μm). Single-mode cw dye and Ti:sapphire lasers are used as pump sources.

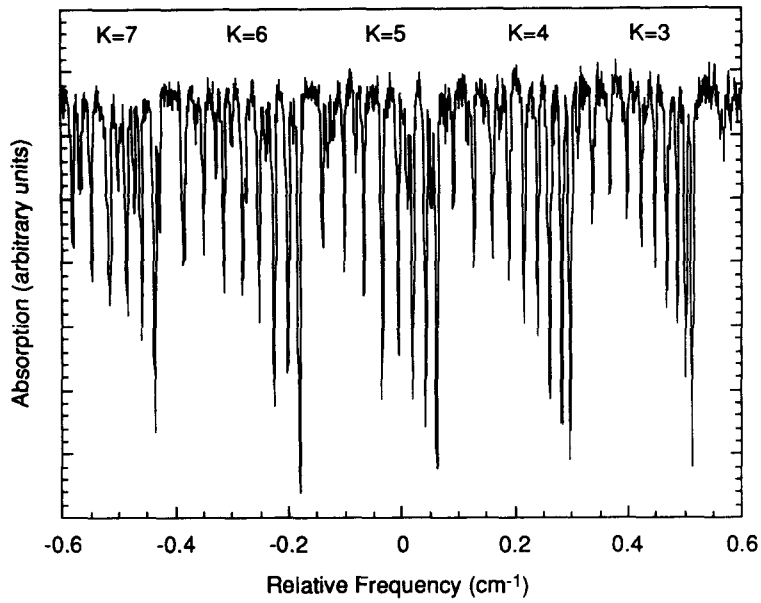

Fig. 2. DOCO ν_2 Q branch near 1850 cm^{-1}.

The 193 nm photolysis of acetic acid, CH_3COOH and CH_3COOD (98% D) produced HOCO and DOCO radicals, respectively. HCCN was generated by the 193 nm photolysis of dibromoacetonitrile, Br_2HCCN. Precursor compounds were introduced into the White cell by gently bubbling He carrier gas through liquid samples. The sample gas mixture and additional He buffer gas flowed through the cell so that their steady-state pressures were typically 300 mtorr and 8 torr, respectively. Gas samples were replenished between every excimer laser pulse. The White cell was adjusted for 24–32 passes, and there was an effective physical overlap between photolysis and probe laser beams of ~28 cm per pass in the middle of the sample cell.

To demonstrate the capabilities of the $AgGaS_2$ DGF spectrometer, we reinvestigated the ν_2 C=O stretching motion of the HOCO and DOCO radicals[8] near 1860 cm^{-1} recently reported by Sears and coworkers.[9] The spectrum in Fig. 2 depicts a portion of the DOCO ν_2 Q branch and illustrates that Doppler-limited resolution was achieved. Line positions and relative intensities are in excellent agreement with those recorded previously using a lead-salt diode laser.[9] Closer inspection suggests that our DFG spectra exhibit slightly better resolution characteristics than the diode laser spectra even though Doppler broadening is the limiting factor in both cases.

Currently, we investigate the ν_2 CCN asymmetric stretching mode spectrum of the HCCN radical.[8] HCCN is especially interesting due to the debate over its equilibrium geometry. High level *ab initio* calculations[10] indicate that the lowest energy structure has an HCC bond angle of 138° while virtually all experimental results[11,12] favor a linear structure. The calculated barrier to linearity ranges from 300 to 800 cm^{-1},[10] suggesting a large amplitude HCC bending motion and possible quasi-linearity in this radical. Very recently, our group has observed the ν_1 CH stretching mode spectrum of this radical using a color center laser spectrometer[13] and found a small barrier to linearity (~100 cm^{-1}) based on the values for ν_4, ν_5 and $2\nu_5$ determined from various hot band series. The ν_2 spectrum should be even more sensitive to the HCCN quasi-linearity, since the *ab initio* structure calculation indicate that the CCN asymmetric stretching motion, CC bond compression and CN bond elongation is strongly coupled to the bend-to-linear transformation.[10]

Infrared matrix studies[12] located the HCCN ν_2 transition at 1735 cm^{-1}. We scanned this area and found numerous transient absorption lines. Figure 3 shows a characteristic 3 cm^{-1} wide segment of this spectrum. HCCN lines were observed throughout the region 1715–1765 cm^{-1}, but

data analysis has been hampered by the large number of overlapping spectral series due to transitions originating from vibrational levels above ground state.

III. DFG WITH III-V DIODE LASERS

Recent advances in single-mode III–V diode laser technology[14] now offer the possibility of employing semiconductor diode lasers as pump sources in DFG. This is particularly attractive as the compact size and ease-of-operation of diode lasers allow the construction of efficient, compact, robust and portable mid-IR spectrometers especially suitable for environmental monitoring of trace species. Potentially, IR radiation from 3 to 6 μm can be generated using type I noncritically phasematched DFG in $AgGaS_2$ and currently available AlGaInP, AlGaAs, InGAs and/or InGaAsP III–V diode lasers.[15] However, the IR power level of all-diode-laser DFG sources has been limited in the past by the relatively low power of commercially available single-mode III–V diode lasers. We reported several nanowatts of cw mid-IR radiation[5] near 5 μm obtained by difference-frequency mixing two visible/near-IR low power laser diodes (2 and 10 mW) in a 45 mm long $AgGaS_2$ crystal. Using KTP as the nonlinear material, Wang and Ohtsu[16] recently generated as much as 300 nW of near-IR radiation ($\sim$1.6 μm) from two diode lasers (50 mW each).

III.1. DFG with high-power semiconductor optical amplifiers

One way to increase the infrared DFG power to a level that is useful for spectroscopic applications is the use of optical semiconductor amplifiers to boost the power of the single-mode diode lasers. Significant progress has been made in obtaining single-mode, diffraction-limited coherent radiation from high-power broad-area and array laser diodes,[17] and more recently, traveling-wave (TW) amplifiers.[18] When seeded by a single-stripe low-power master diode laser,[18] the semiconductor amplifiers have been demonstrated to generate near-diffraction-limited, single-longitudinal mode emission required for applications such as nonlinear frequency conversion through second harmonic generation,[19] or sum-frequency generation.[20] Under pulsed operation 11.6 W of peak power was generated by a broad-area amplifier seeded with a laser diode.[18] Recently, 5.25 W of cw emission[21] was obtained from a tapered strip[18,22] GaAlAs amplifier seeded by a $Ti:Al_2O_3$ laser.

We demonstrated difference-frequency mixing of a high-power GaAlAs tapered traveling-wave semiconductor amplifier[6] with a cw $Ti:Al_2O_3$ laser in a 45 mm long $AgGaS_2$ crystal cut for type

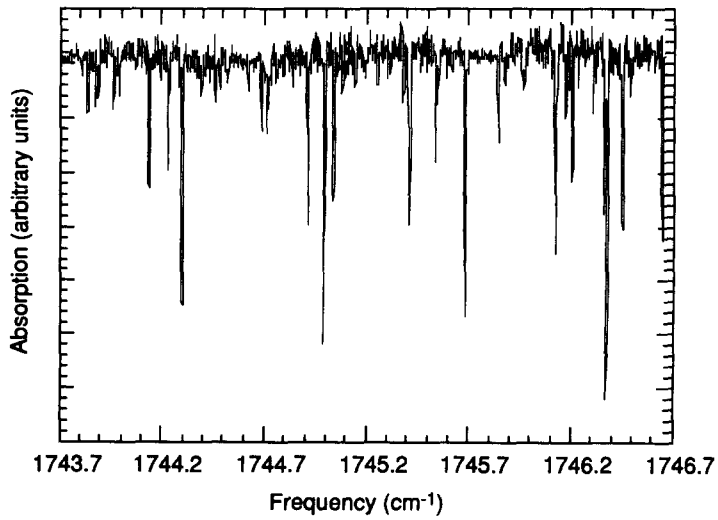

Fig. 3. A 3 cm^{-1} portion of the HCCN ν_2 CCN antisymmetric stretching mode spectrum.

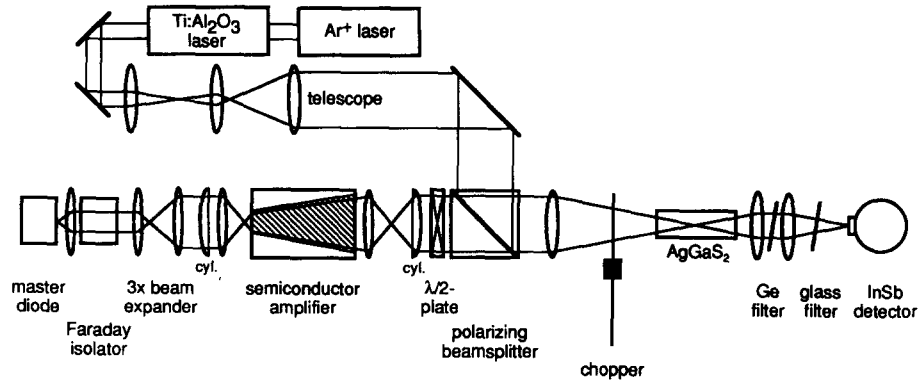

Fig. 4. Experimental setup used to mix the outputs of a GaAlAs tapered amplifier and a Ti:Al_2O_3 laser in $AgGaS_2$ cut for 90° type I phasematching. The amplifier was seeded by a cw single-mode laser diode.

I 90° phasematching at room temperature (Fig. 4). The master laser was an index-guided diode laser (SDL Inc., Model SDL5410C) emitting up to 130 mW in a single-mode near 860 nm with a less than 30 MHz linewidth. By changing the temperature, its wavelength was tunable over ~1–2 nm. The amplifier chip was bonded active side down on a heatsink which in turn was attached to a water-cooled fixture and allowed unobstructred optical access to both facets. After collimation by a $f = 2.0$ mm lens (0.5 NA), the master laser power passed through a Faraday isolator, and a 3 × beam expander. Final coupling of the injected signal into the amplifier was accomplished by a combination of a closely spaced $f = 15$ cm cylindrical lens and a high numerical aperture $f = 7.7$ mm lens. The cylindrical lens served to move the focused point of the input beam to several-hundred μm in front of the facet in the junction plane, while allowing it to coincide with the facet in the perpendicular plane. This highly astigmatic input resulted in a Gaussian input beam width of approx. 150 μm in the junction plane and 1 μm in the perpendicular plane. With 100 mW of master laser power incident on the amplifier, 38 mW was coupled into the amplifier. The GaAlAs tapered amplifier used in this work is characterized by a 250 μm input width, 500 μm output width, 1.5 mm length, and a single quantum well separate confinement heterostructure active region. At high currents the amplifier had a peak gain near 860 nm. The facets of the amplifier were antireflection coated at 860 nm for single-pass traveling-wave operation. A second $f = 7.7$ mm lens was used to collimate the amplifier emission, perpendicular to the junction. In the junction plane, the emission was brought to a focus by the $f = 7.7$ mm lens, and collimated by a $f = 10$ cm cylindrical lens.

The pump wave was provided by a cw Ti:Al_2O_3 ring laser (Coherent Moel 899-21) operated at 715 nm. Pump and signal wave polarizations were chosen perpendicular for 90° type I phase-matching in $AgGaS_2$. Both beams were overlapped and focused into the 45 mm long $AgGaS_2$ crystal. A three-lens telescope design in the pump laser beam path allowed matching of beam waist widths for the two beams at the center of the crystal. The beamwaists were set of ~33 μm in both vertical and horizontal planes, close to optimum focusing. As measured with a beam profiler, the spatial distribution of pump and signal beams was near-Gaussian, where in the case of the signal wave (amplifier) approx. 20% of the focused light was in sidelobes outside the main Gaussian envelope.

A maximum signal wave power of 1.5 W was obtained under cw operation and 3.2 W under pulsed operation with 50-μs-long pulses and 0.1% duty cycle. After correcting for the 75% capture efficiency of the $f = 7.7$ mm lens and transmission losses of the beamsplitter and other optical components, the actual amplifier output at the maximum cw current of 6 A was 2.5 W. The maximum operating currents for the amplifier were arbitrarily chosen and do not represent a fundamental operating limit of the amplifier.

The difference-frequency radiation generated in the $AgGaS_2$ crystal was collimated and focused

on a liquid-N_2-cooled photovoltaic InSb detector. A Ge filter was used to block pump and signal waves and transmit the DFG radiation. Phasematching was found at 714.60 and 858.60 nm for pump and signal wavelengths, respectively, corresponding to a difference-frequency wavelength of $\sim 4.26\,\mu$m (2350 cm^{-1}). Tuning of the IR wavelength was limited to ~ 25 cm^{-1} by the limited temperature tuning range of the master diode laser.

Figure 5 shows the generated infrared DFG power as a function of the diode amplifier output power for cw and pulsed amplifier operation. Values shown are corrected for the 4.3 μm transmission loss of the optical components between the crystal and detector, but not for the 17% Fresnel reflection at the crystal output facet. For all measurements the Ti:Al_2O_3 laser output was fixed at a cw power of ~ 330 mW, and the diode amplifier output power was changed by varying the pump current. The dotted line indicates the low-power external slope efficiency of $\sim 35\,\mu$W/W for the DFG process. Maximum DFG powers of 47 and 89 μW were obtained for the cw and pulsed operation, respectively. The drop in experimental slope efficiency at high amplifier power levels is attributed to the degradation in the diode laser beam quality occurring at highest amplifier currents. To evaluate the contribution of thermal effects in the mixing crystal to the drop in slope efficiency at high amplifier power levels the absorption loss in the $AgGaS_2$ crystal was determined at 858 nm. From the ratio of transmitted to reflected signal power we found the absorption in $AgGaS_2$ at 858 nm to be as low as $\sim 1.5\%$ cm^{-1}. At high diode power levels, no decay of the IR pulse amplitude during the 50 μs pulse was observed, indicating that thermal lensing did not contribute to the drop in experimental slope efficiency occurring at the highest pulsed powers. Correction for the Fresnel reflection losses for pump, signal and idler waves at the surfaces of the uncoated $AgGaS_2$ crystal, the Ge filter and the CaF_2 lenses, results in an internal slope efficiency of $\sim 65\,\mu$W/W at 330 mW cw Ti:Al_2O_3 pump power.

III.2. Cavity-enhanced DFG scheme using diode lasers

Alternatively, the infrared DFG power can be increased by making use of the high circulating fields present inside optical resonators by placing the nonlinear crystal either in an external (passive) enhancement cavity or in one of the pump laser cavities.[23]

We have built a DFG source that uses a tunable extended-cavity diode laser (ECDL) near 795 nm (500 kHz linewidth), a diode-pumped Nd:YAG laser at 1064 nm (5 kHz linewidth) and an external ring enhancement cavity around a $AgGaS_2$ crystal. The enhancement cavity resonates the signal wavelength (Nd:YAG laser) thereby increasing the signal power present inside the mixing crystal.

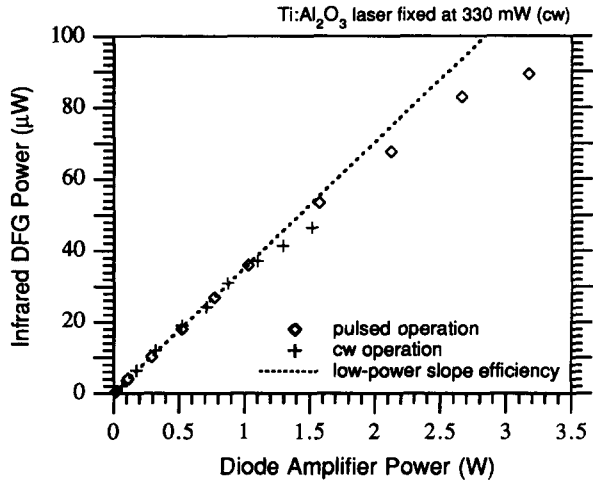

Fig. 5. Infrared DFG $\lambda \approx 4.3\,\mu$m power as a function of the amplifier power incident on the crystal for cw and pulsed modes of operation. The Ti:Al_2O_3 laser cw power was fixed at 330 mW.

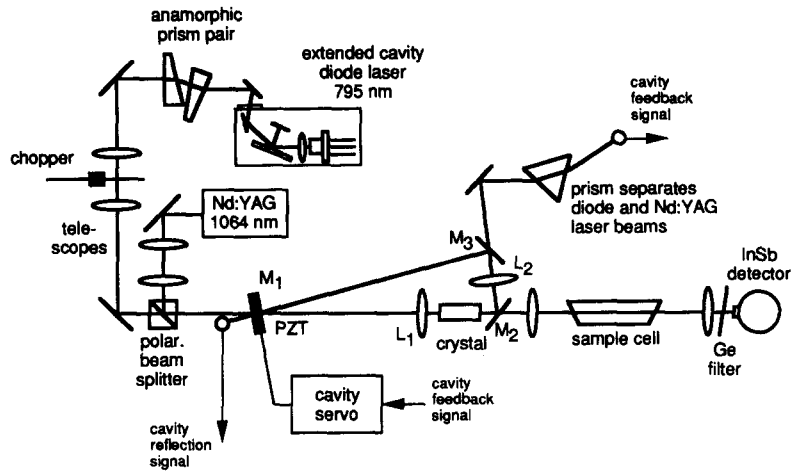

Fig. 6. Experimental setup used to mix the outputs of an ECDL near 795 nm and a diode-laser-pumped Nd:YAG laser at 1064 nm in $AgGaS_2$ cut for 90° type I phasematching. The Nd:YAG laser radiation inside the mixing crystal is resonantly enhanced by using a three-mirror ring build-up cavity.

The IR power scales as the product of the signal and pump powers and hence its enhancement depends linearly on the buildup factor.

The experimental diagram in Fig. 6 shows the ring build-up cavity, the extended-cavity-diode laser, and the diode-pumped Nd:YAG laser. The ECDL[14] uses an index-guided, quantum-well laser (SDL, Inc., Model SDL5410C, 100 mW), a 0.60 NA collimating objective, and a mirror and grating (2400 lines/mm) used in the Littman configuration. To improve the tuning characteristics of the ECDL the output facet of the laser chip was antireflectance (AR) coated with Al_2O_3 and HfO_2. Most high-power diode lasers are supplied from the manufacturer with reduced reflectance coatings on the front facet and high reflectance (HR) coatings on the back facet. These standard high-power lasers will work well in an ECDL configuration but further reduction of the front facet reflectance allows a broader tuning range. An anamorphic prism pair (6×) and a telescope were used to approximately match the spatial mode of the ECDL to the Nd:YAG laser mode in the ring build-up resonator.

The signal wave was provided by a cw diode-pumped monolithic Nd:YAG ring laser (Lightwave Electronics, Inc., Model 122-1064-500-F, 500 mW) at 1064 nm. Pump and signal wave polarizations were perpendicular for type I phasematching in $AgGaS_2$. Both beams were spatially overlapped with a polarizing beam splitter. Telescopes were used in both beam paths to match the beam waists at the center of the crystal. The beam waists were set to $\sim 20\,\mu$m in both vertical and horizontal planes, which is close to optimum focusing.[3]

To minimize the impact of thermal effects on the nonlinear conversion efficiency the signal wave at 1064 nm rather than the pump wave at 795 nm was resonated in the build-up cavity. Due to a poor thermal conductivity ($\sim 0.115\ \mathrm{Wcm^{-1}\,^{\circ}C^{-1}}$), $AgGaS_2$ suffers from thermal lensing problems especially if high-power pump sources at wavelengths close to the absorption band edge of the material (~ 500 nm) are used.[24] Both, to avoid degradation of the wavefronts by thermal lensing effects and to have a broad angle tuning range a short $AgGaS_2$ mixing crystal (5 mm long) was chosen in this experiment. After applying AR-coatings to the crystal facets the total linear absorption loss of the $AgGaS_2$ crystal at 1064 nm was measured to be $\sim 1.5\%$.

The ring build-up cavity consisted of three flat mirrors (M_1–M_3) and two intracavity-lenses ($f_{L_1} = 50$ mm, $f_{L_2} = 25$ mm) together with a 5 mm long $AgGaS_2$ crystal cut for type I 90° phasematching. With a crystal aperture of 5 mm this configuration allowed to access internal phasematching angles between 90 and 67°. The total length of the ring cavity was ~ 28 cm with the full angle Θ on mirror M_1 being $\sim 3°$. The facets of the nonlinear mixing crystal were coated

with a single-layer Al_2O_3-antireflectance-coating for low loss at 1064 nm ($R \approx 4 \times 10^{-5}$). In spite of the quality of the coatings, passive losses from the lenses ($R < 0.25\%$/surface, nominally) reduced the cavity build-up. However, the cavity setup shown in Fig. 6 could be realized almost exclusively with standard Nd:YAG laser optics. Mirrors M_2 and M_3 were HR-coated (nominally $R \sim 98.5\%$ and $R \sim 99.7\%$, respectively) for s-polarized light at 1064 nm. The IR radiation generated inside the crystal was coupled out through mirror M_2 which was an Al_2O_3-substrate HR-coated for 1064 nm with a transmission $T \approx 78\%$ for the generated difference-frequency radiation near 3 μm. Mirror M_1 was used as the input coupler with $T \approx 4\%$ (nominally) at 1064 nm chosen to impedance-match[25] the build-up cavity to the signal wave losses. Approximately 85% of the diode laser power at 795 nm incident on the cavity could be coupled through M_1.

With no mixing crystal inside the buildup cavity approx. 75% of the incident Nd:YAG laser power was coupled into the cavity and enhanced by a factor of ~ 24.5 corresponding to a total cavity round-trip-loss of $\sim 4.1\%$. After introducing the crystal into the cavity the coupling increased to $\sim 83\%$, indicating a better match of the input coupler transmission and the total cavity round-trip-loss. However, due to the additional absorption of the mixing crystal the buildup factor decreased to ~ 14.5 corresponding to a total cavity round-trip loss of $\sim 6.9\%$.

The coupling efficiency of the Nd:YAG laser power into the build-up cavity was determined from the power reflected off the input coupler M_1 while the build-up cavity was tuned over the resonance with the PZT-driven mirror M_1. The circulating power inside the cavity could be inferred from the Nd:YAG laser power which leaked through mirror M_3. After traversing a 60° prism to separate the Nd:YAG laser beam form the diode laser beam the transmitted signal was also used to lock the cavity resonance to the Nd:YAG laser frequency with a standard modulation control scheme.

The DFG radiation generated in the $AgGaS_2$ crystal was collimated outside the build-up cavity with a CaF_2 lens (5 cm focal length) and then detected by a liquid-N_2-cooled photovoltaic InSb detector (1 mm dia sensitive area; factory calibrated responsitivity of ~ 1.248 A/W at 3μm). A broad-band antireflection-coated Ge filter was used to block pump and signal waves while transmitting the 3 μm-difference-frequency radiation. Using 1064.504 nm as the signal wave we found type I 90° phasematching at a diode laser wavelength of 795.5 nm, corresponding to a difference-frequency wavelength of ~ 3.148 μm (3176.7 cm^{-1}). The laser wavelengths were determined with a spectral resolution of ~ 30 MHz and an absolute accuracy of ~ 500 MHz by coupling the radiation via a single-mode probe fiber into a Lambdameter.[26] The DFG phasematching bandwidth at a phasematching angle of 90° is shown in Fig. 7. This was recorded by tuning the wavelength of the ECDL. The large phasematching bandwidth of ~ 8.8 cm^{-1} (FWHM) is in good agreement with the theoretically calculated value of 8.1 cm^{-1} which mainly results from the short length (5 mm) of the nonlinear optical mixing crystal.

Figure 8 depicts the mid-IR DFG power at 90° phasematching for a fixed diode laser power of 12.1 mW (measured after the input coupler of the build-up cavity) as a function of the Nd:YAG laser power incident on the enhancement cavity. The Nd:YAG laser power was varied by the relative angle between a polarization rotator and an analyzer. Values shown are corrected for the 3 μm transmission loss of the optical components external to the cavity ($T \approx 89\%$), but not for the transmission loss of IR light in the output coupler of the build-up cavity ($T \approx 78\%$). The plot shows the expected linear dependence of the generated IR power on the signal power. However, the experimentally determined slope efficiency of ~ 4.1 nW/mW at 12.1 mW diode laser power is approx. 4 times less than the value which was predicted based on the theoretical model [given in Refs (3, 4)] assuming ideal Gaussian beams and an effective nonlinear coefficient of 12×10^{-12} m/V for type I 90° phasematching in $AgGaS_2$. This deviation between experiment and theory was also found in previous $AgGaS_2$-DFG experiments.[6] A maximum cw DFG power of ~ 1.7 μW was obtained after the external cavity with ~ 13.6 mW of diode laser power and 360 mW of Nd:YAG laser power. Taking into account the build-up cavity output coupler transmission at 3 μm, this corresponds to ~ 2.1 μW of DFG power after the mixing crystal. Even at the high signal power

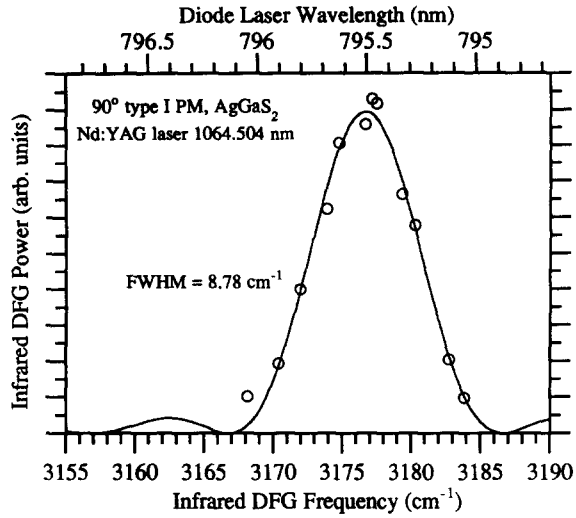

Fig. 7. Phasematching bandwidth of the DFG mixing process at a phasematching angle of 90° recorded by tuning the diode laser wavelength. The large bandwidth of $>8\,cm^{-1}$ (FWHM) is due to the 5 mm length of the used nonlinear optical mixing crystal.

levels circulating inside the build-up cavity the IR DFG power was the same for both, cw and pulsed modes of operation. For cw operation the build-up cavity resonance was locked to the Nd:YAG laser while pulsed operation was obtained by sweeping the cavity over its resonance in ~ 0.4 ms and detecting the transmitted IR. This indicates that even at circulating power levels of >3.5 W inside the cavity no degradation of the nonlinear conversion efficiency due to thermal lensing effects was observed.

By tuning the wavelength of the ECDL from 795 to 812 nm (over ~ 17 nm) and adjusting the phasematching angle of the mixing crystal (over $\sim 15°$) the IR wavelength could be tuned from 3.155 to 3.423 μm (3170–2921 cm^{-1}). Figure 9 shows the relative IR DFG power as a function of the diode laser and IR wavelengths over the entire tuning range of the diode laser. The tuning curve was recorded by setting the phasematching angle to a given value and tuning the diode laser over the DFG phasematching bandwidth. The DFG power levels shown here are normalized to

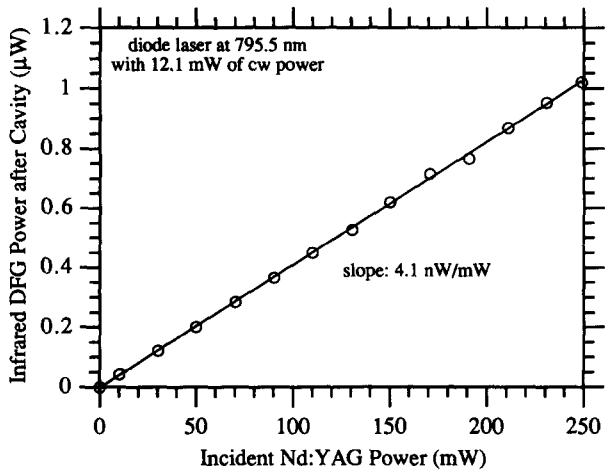

Fig. 8. Generated IR DFG power as a function of the Nd:YAG laser power incident on the enhancement cavity. During this measurement, the diode laser power was fixed at 12.1 mW (measured after the input coupler of the build-up cavity). Values shown are corrected for transmission losses of the optical components external to the build-up cavity at a wavelength of 3 μm.

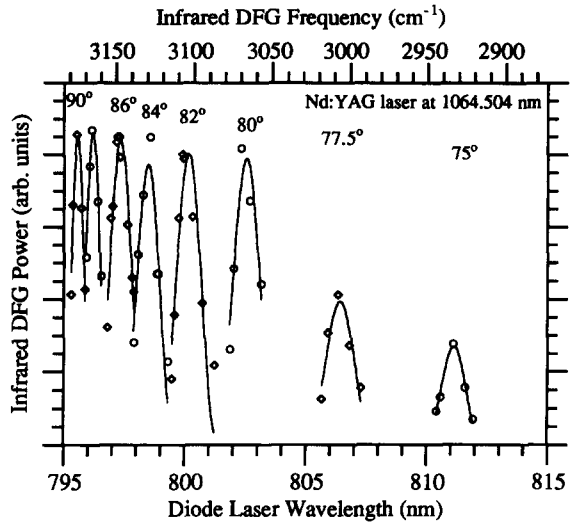

Fig. 9. Tuning range and power output of the IR DFG radiation. Infrared tuning was accomplished by varying the wavelength of the diode laser for a given orientation of the mixing crystal.

the incident diode laser power which varied from 10 to 15 mW over this tuning range. Continuous mode-hop-free IR tuning ranges of > 40 GHz were achieved by scanning the PZT on the ECDL. Figure 9 indicates that for phasematching angles above 80° the effective phasematching length[27] is actually larger than the physical length of the mixing crystal which results in a nearly constant IR DFG power between 90 and 80°. For phasematching angles smaller than 80° the effective phasematching length drops below the physical length of the crystal due to walk-off effects resulting in an equivalent drop of the generated IR power.

To demonstrate the applicability of this compact all-solid-state DFG source a portion of the absorption spectrum of the fundamental ν_3-asymmetric stretch vibration of methane (CH_4) around

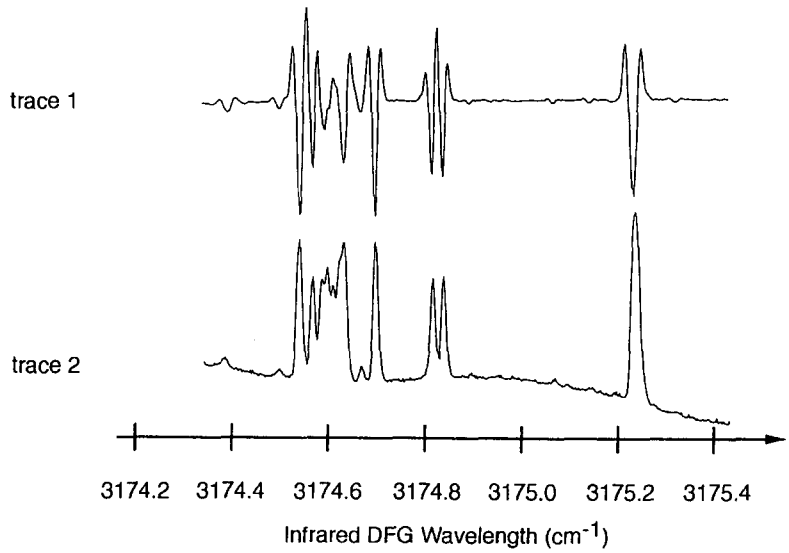

Fig. 10. Methane absorption spectrum near 3.2 μm (fundamental ν_3-asymmetric stretching motion) using a 50-cm-long absorption cell and a methane pressure of ~ 10 torr; trace 2 a direct absorption signal obtained by averaging 10 sweeps; trace 1, $2f$-absorption signal (single sweep) recorded with a lock-in amplifier. The spectrum was recorded at a phasematching angle of 90° by tuning the diode laser wavelength over a 30 GHz portion of the phasematching bandwidth.

3.2 μm was recorded (see Fig. 10). The phasematching angle was set to 90° and the ECDL wavelength was tuned over a ~30 GHz portion of the DFG phasematching bandwidth. Only 100 mW of incident Nd:YAG laser power was used to record this spectrum and corresponds to an IR power level of ~0.45 μW. The methane pressure in the 50 cm long absorption cell was set to the vapor pressure of methane at 77 K (1333 Pa, 10 torr) by using a liquid-N_2-cooled reservoir. Figure 10 depicts a portion of the recorded methane absorption spectrum and demonstrates the high signal-to-noise levels which could readily be obtained. Trace 1 shows a (single sweep) background-free absorption spectrum recorded by wavelength-modulating the diode laser (cavity length) and detecting the 2f-absorption signal using lock-in techniques. Trace 2 shows the direct absorption spectrum of the same lines recorded with a digital oscilloscope averaging 10 sweeps.

IV. CONCLUSIONS

In conclusion, DFG in $AgGaS_2$ utilizing dye/Ti:Al_2O_3, diode/diode, diode/Ti:Al_2O_3 and diode/Nd:YAG laser input configurations has been demonstrated, producing tunable mid-IR radiation for molecular spectroscopy.

DFG schemes using visible/near-IR diode lasers as pump sources are attractive since they allow the construction of compact portable spectroscopic laser sources for wide range of applications. Techniques to increase the IR power levels such as the use of high-power optical amplifiers or external build-up cavities have been explored. The generated IR power levels of 2–50 μW are sufficient for sensitive IR absorption spectroscopy. The compact cavity-enhanced IR DFG source (footprint of 0.5 m^2) could be tuned from 3.155 to 3.423 μm (3170–2921 cm^{-1}) and will be an attractive tool for wide range of spectroscopic applications whenever low power consumption and no-water-cooling are important and for wavelength regions where high-power GaAlAs optical amplifiers[6] are not available.

Acknowledgements—This work has been supported by NSF and the Robert A. Welch Foundation. The authors like to thank C. E. Miller, W. C. Eckhoff and R. F. Curl, (Rice University, Houston, TX), L. Goldberg (NRL, Washington, DC), S. Waltman and L. Hollberg (NIST, Boulder, CO) and J. L. Hall (JILA, Boulder, CO) for contributions to this work. They also like to thank Lightwave Electronics, Inc. for providing the diode-pumped Nd:YAG laser used in this work. U. Simon gratefully acknowledges the support of the A. v. Humboldt Foundation by a F. Lynen Fellowship.

REFERENCES

1. A. S. Pine, *J. Opt. Soc. Am.* **64,** 1683 (1974).
2. M. G. Bawendi, B. D. Rehfuss and T. Oka, *J. Chem. Phys.* **93,** 6210 (1990).
3. P. Canarelli, Z. Benko, R. F. Curl and F. K. Tittel, *J. Opt. Soc. Am. B* **9,** 197 (1992).
4. A. H. Hielscher, C. E. Miller, D. C. Bayard, U. Simon, K. P. Smolka, R. F. Curl and F. K. Tittel, *J. Opt. Soc. Am. B* **9,** 1962 (1992).
5. U. Simon, C. E. Miller, C. C. Bradley, H. G. Hulet, R. F. Curl and F. K. Tittel, *Opt. Lett.* **18,** 1062 (1993).
6. U. Simon, F. K. Tittel and L. Goldberg, *Opt. Lett.* **18,** (1993).
7. K. Unfried *et al.*, *J. Mol. Spectrosc.* **150,** 86 (1991); R. F. Curl *et al.*, *Chem. Phys. Lett.* **161,** 98 (1992); J. W. Stevens *et al.*, *J. Mol. Struct.* **190,** 41 (1988).
8. C. E. Miller, U. Simon, W. C. Eckhoff, R. F. Curl, F. K. Tittel, In *AIP Conference Proc.* 290, pp. 122–127. AIP Press, New York (1994).
9. T. J. Sears, W. M. Fawzy and P. M. Johnson, *J. Chem. Phys.* **97,** 3996 (1992).
10. P.-A. Malmquist, R. Lindh, B. O. Ross and S. Ross, *Theor. Chim. Acta* **73,** 155 (1988); E. T. Seidl and H. F. Schaefer, III, *J. Chem. Phys.* **96,** 4449 (1992); and extensive experimental and theoretical references therein.
11. S. Saito, Y. Endo and E. Hirota, *J. Chem. Phys.* **80,** 1427 (1984); F. X. Brown, S. Saito and S. Yamamoto, *J. Mol. Spectrosc.* **143,** 203 (1990).
12. A. Dendramis and G. E. Leroi, *J. Chem. Phys.* **66,** 4334 (1977).
13. C. L. Morter, S. K. Farhat and R. F. Curl, *Chem. Phys. Lett.* **207,** 153 (1993).
14. C. E. Wieman and L. Hollberg, *Rev. Sci. Instrum.* **62,** 1 (1991).
15. K. Nakagawa, M. Ohtsu, C. H. Shin, M. Kourogi and Y. Kikunaga, *Laser Spectroscopy* (*Tenicols* '91) (Edited by M. Ducloy), pp. 353–358. World Scientific, Singapore (1992).
16. W. Wang and M. Ohtsu, *Opt. Comm.* **102,** 304 (1993).

17. L. Goldberg and J. F. Weller, *Appl. Phys. Lett.* **50,** 1713 (1987); L. Goldberg and M. K. Chun, *Appl. Phys. Lett.* **53,** 1900 (1988).
18. L. Goldberg, D. Mehuys, M. R. Surette and D. C. Hall, *IEEE J. Quantum Electron.* **QE-29,** 2029 (1993).
19. L. Busse, L. Goldberg and D. Mehuys, *Electron. Lett.* **29,** 77 (1993).
20. L. Goldberg, M. K. Chun, I. N. Duling, III and T. F. Carruthers, *Appl. Phys. Lett.* **56,** 2071 (1990).
21. D. Mehuys, L. Goldberg and D. Welch, *IEEE Photonics Tech. Lett.* **5,** 1179 (1993).
22. J. N. Walpole, E. S. Kintzer, S. R. Chinn, C. A. Wang and L. J. Misaggia, *Appl. Phys. Lett.* **61,** 740 (1992).
23. F. J. Effenberger and G. J. Dixon, In *Digest of Topical Meeting on Advanced Solid State Lasers, p.* 59. Optical Society of America, Washington, DC (1992).
24. C. E. Miller, W. C. Eckhoff, U. Simon, F. K. Tittel and R. F. Curl, *SPIE, OE/LASE* '94, Los Angeles, CA, January (1994).
25. W. J. Kozlovsky, C. D. Nabors and R. L. Byer, *J. Quantum Electron.* **QE-24,** 913 (1988).
26. J. L. Hall and S. A. Lee, *Appl. Phys. Lett.* **29,** 367 (1976).
27. R. L. Byer and R. L. Herbst, Parametric Oscillation and Mixing. In *Nonlinear Infrared Generation* (Edited by V. R. Shen). Springer-Verlag, New York (1977).